VI-2 THE ROLE OF CROSS-SLIP IN BRITTLE FRACTURE AND FATIGUE

A. J. McEvily Jr.[1] and T. L. Johnston[2]

ABSTRACT

The relationship between slip character and resistance to cracking under unidirectional and cyclic loading conditions is discussed for those single phase solids free from interstitial effects. Slip character is viewed in terms of the appearance of slip bands as revealed topographically by light microscopy and in terms of the form and distribution of dislocations as revealed by electron transmission microscopy. The controlling process is considered to be cross slip which can be correlated to the rate of unidirectional strain hardening.

Increased difficulty of cross slip intensifies strain within glide bands, induces planar glide, increases the slope of the yield stress grain size dependence and thereby increases the probability of crack formation. Examples are given where changes in slip character override the importance of the temperature dependence of the yield stress in the determination of the ductile to brittle transition.

In contrast, cross slip promotes the process leading to fracture under cyclic loading conditions. Examples are given of the influence of ease of cross slip on the development of slip band topography and the nucleation of cracks. It is pointed out that a reduction in stacking fault energy can lead to an increase in resistance to fatigue, but relative to the macroscopic yield strength of homogeneous materials there may be no apparent improvement except in cases where cyclic hardening is pronounced.

The growth of fatigue cracks is related to slip character primarily through the effect of slip on strain hardening. The effects of plane strain, plane stress, and strain amplitude on the crack growth are discussed. A generalized expression for the rate of crack growth is given which is related to the fourth power of a stress intensity parameter and the unidirectional material properties and is shown to be in agreement with experimental results.

1,2 Scientific Laboratory, Ford Motor Company, Dearborn, Michigan

INTRODUCTION

The recognition that cracks are formed in crystalline solids as a consequence of plastically induced stress or strain concentrations, carries with it the implication that the nature and distribution of plastic flow at the onset of yielding can have a controlling influence on the stress and strain at fracture. In fact, there is now good experimental evidence, obtained with ionic solids,[1][2][3] alloys capable of order-disorder transitions[4][5] and iron-base solid solutions,[6][7] that the character of plastic deformation (by glide) does indeed determine fracture behavior under both unidirectional and cyclic loading conditions.

The aim of the present paper is to review the relationships between slip character and resistance to fracture. A description will be given of slip character in terms of surface topography, dislocation configuration and cross slip, followed by a consideration of the effect of the propensity for cross slip on the rate of strain hardening in the early stages of deformation of polycrystals. The relevance of slip behavior to the formation of cleavage cracks will then be discussed in materials where interstitial locking of dislocation sources and second phase particle effects are absent. Finally, the interplay between slip character and fatigue phenomena will be described.

SLIP CHARACTER

It is convenient to qualify what is meant by slip character by referring to specific examples. For instance, the slip bands in an iron-3¼% silicon alloy beryllium and magnesium oxide deformed at low temperatures appear planar when viewed in a conventional light microscope, i.e., each slip band trace in the surface is straight. In contrast, the slip band appearance in pure iron and silver chloride deformed at room temperature is wavy. For these examples there is a clear and straightforward distinction in slip character as shown in figure 1. However, conventional microscopy may not be sufficiently discriminating in those situations where slip traces are more or less similar, but there are subtle differences in the fine topographical structure of the slip bands. A better assessment of slip character can be obtained through the use of electron transmission microscopy. In this case the basis for comparison lies in the arrangement and configuration of dislocations within glide bands. For example, we may observe cells of densely tangled and jogged dislocations containing many dipoles as

shown in figure 2a; or, in contrast, the dislocation arrangement may be characterized by long straighter segments which are distributed in a more uniform manner as in figure 2b.

Even though there is no clear cut spatial correlation between internal dislocation arrangement and surface displacements, it is possible to relate qualitatively both the changes in slip band appearance and dislocation structure to changes in dislocation behavior. The particular process which we feel is of fundamental importance is the spreading of slip from primary slip planes to secondary systems within a glide band. The mechanism that appears to be most significant is the cross slip of screw dislocations. The more easily this process occurs the glide bands tend to become more diffuse because deformation can spread in directions out of primary glide planes. For a given plastic strain, the average shear strain within each band is less, the greater the propensity for cross slip. In terms of dislocation arrangements, there is good evidence that cell formation, consisting of tangled jogged dislocations, is associated with the ability to cross slip, whereas straight uniformly distributed dislocations reflect more difficult cross slip.[8]

In the fcc lattice, the rate controlling feature of cross slip is the transfer of a screw dislocation from one {111} system to another {111}; this probably depends upon the constriction of extended dislocations which in turn is a function of stress, temperature and stacking fault energy. The velocity on the secondary {111} system is a function only of the locally resolved shear stress. However, in the bcc lattice wavy glide requires cross slip of screw dislocations from {110} planes onto {123} and {112} and in the rock salt structure, wavy slip requires cross slip between {110} systems and {100} and {112}. In these cases, the relative velocities of dislocations on the respective planes control the cross slip processes that determine slip character.

In many ordered alloys, glide is accomplished through the motion of superlattice dislocations that consist of two unit dislocations connected by an anti-phase domain boundary. The separation of the two unit dislocations increases as the ordering energy decreases. It has been found[9][10] that in many ordered alloys (Cu_3Au, Fe-Co) slip is planar. The reason for this is that if the leading unit dislocation cross slips out of the plane because of a local stress concentration, the trailing dislocation senses the superposed repulsive fields of both the leading dislocation and the obstacle which caused the initial cross slip. As a consequence, the trailing dislocation leaves the glide plane not at the same point as the leading dislocation. The total superlattice dislocation does not lie on the cross slip plane and therefore cannot move very far. The possibility of non-coordinated cross slip, therefore, decreases the frequency of a superlattice dislocation cross-slipping as a whole onto a neighboring plane.

CROSS SLIP AND STRAIN HARDENING IN POLYCRYSTALS

An important aspect of the fracture of single phase polycrystalline aggregates is the stress dependence of the propagation of plastic flow from one grain to another. In general terms, the significant factor here is the effect of grain boundaries on the strain hardening rate in both the micro and macro stages of plastic deformation. Recent studies have shown experimentally that any factor, such as alloying or a change in degree of order, or a reduction in temperature, that decreases the ability to cross-slip (manifested e.g. in terms of uniform distribution of straight dislocation segments) increases the strain hardening rate of a polycrystal. For example Ku et al[11] found that aluminum in solution (which lowers the stacking fault-energy of copper) has only a small effect on the micro yield stress of a series of copper-base polycrystals. However, the addition of aluminum significantly increases the grain boundary contribution to the macroscopic flow stresses, as shown in figure 3. In other words, the restriction of cross slip has increased the initial strain hardening rate. Thomas[12] has also pointed out that a decrease in stacking fault energy increases the yield stress of α-brasses. Related observations have been made in iron-base solid solutions, namely Fe-V and Fe-Co;[6] these solutes were shown to change the dislocation distribution from tangled cells to more uniform tangle segments, and also to increase the initial rates of strain hardening of polycrystals.

A decrease in temperature has an analogous effect in that dislocations in deformed material become more uniformly distributed and less prone to form a cellular structure[13][14]. The increased macroyield stress appears to reflect in part, the increased difficulty of cross slip and the consequent increase in the rate of strain hardening[6][15].

The extent to which the ability to cross slip influences the initial rate of strain hardening may be assessed by using the approach of Armstrong et al[16] as a frame of reference. For a given plastic strain, the maximum shear stress, τ, that a region containing a slip band can sustain in a polycrystal of grain size ℓ, is given by

$$\tau = \tau_o + k_s \ell^{-\frac{1}{2}} \qquad (1)$$

where τ_o is the shear stress necessary to generate the slip band in a crystal having no surface constraints of similar orientation with respect to the direction of the applied stress. At some arbitrary small strain, τ_o, will include the additional stress that reflects the necessity for a slip band to cut through other slip bands formed as a consequence of multiple slip. $k_s \ell^{-\frac{1}{2}}$ is the extra shear stress that must be imposed to generate slip in the neighboring grain at each end of the slip band from dislocation sources at or near the boundary.

For a randomly oriented polycrystal, the operable slip systems in the neighboring grain will not, in general, lie in the plane of maximum shear stress provided by the above slip band. Furthermore, since 5 independent slip systems are required to enable each grain of a polycrystal to deform macroscopically (Von Mises-Taylor criterion), more than one slip system must operate in the neighboring grain to accommodate the displacement associated with each impinging slip band. The number of slip systems required can range from 1 or 2 for a simple tilt boundary, to five systems for misorientations involving large angles of tilt and twist. Armstrong et al showed that for a planar slip band, k_s is proportional to $m\tau_c$, where m is an average orientation factor that is appropriate for the generation of the necessary number of slip systems in the neighboring grains; τ_c is the shear stress necessary to generate dislocations from sources at or near the boundary.

The value of k_s depends upon the plastic anisotropy of the solid in question; it decreases as the number of available independent slip systems increases and as the ability to cross slip increases. The possible effects of easy cross slip may be suggested: a) the production of broader and more diffuse glide bands which impinge upon larger areas of intergranular surfaces increases the probability of encompassing dislocation sources in the grain boundaries; b) a single dislocation source will be able to activate two independent slip systems in neighboring grains at lower stresses than if cross slip were difficult. This latter effect is closely related to reduction in the stress dependence of dislocation multiplication which is most important in the determination of the macroscopic yield stress (i.e., a plastic strain of 10^{-3}). Certain solids are more plastically anisotropic at low temperatures, e.g., hcp metals zinc, beryllium, etc., and rock salt solids like sodium chloride and, therefore, manifest stronger grain boundary strengthening effects at low temperatures. Armahan et al[7] showed that the flow stress of AgCl was sensitive to grain size at 77°K, because the deformation was planar, confined by and large to the {110} system. At room temperature, however, silver chloride deforms by wavy glide in which screws can freely cross slip between {110} {100} and {111} planes; at this temperature grain size had a very small influence on the flow stress. Groves and Kelly[18] have calculated the number of independent systems available in different crystal structures, they found that for the rock salt structure, if slip is confined exclusively to {110} planes, the number of independent systems is only 2; similarly, for slip confined to the basal planes of hcp metals, the number of independent slip systems is only 2. Under these conditions grain boundary hardening is very pronounced since the Von-Mises criterion is not readily obeyed and because high applied stresses are needed to propagate slip, such materials are essentially brittle.

In summary, therefore, slip character is viewed in terms of the appearance of slip bands as revealed topographically by light microscopy and in terms of the distribution and form of dislocations as revealed by transmission electron microscopy, as shown in Table I. The controlling process is considered to be cross slip which has been correlated to the rate of unidirectional strain hardening of polycrystals.

CROSS SLIP AND BRITTLE FRACTURE

It is self evident that any process that restricts tensile stress concentration generated by plastic flow will reduce the probability of crack formation. In a polycrystal the most critical sites of high tensile stress are at the tips of blocked glide bands, as at grain boundaries. The magnitude of such stress concentrations increases with the effective plastic displacements associated with blocked glide zones; these displacements increase with grain size and the strength of the grain boundary as a barrier to slip propagation (i.e., the values of k_s). An increase in the number of slip systems and in the ease of cross slip will therefore decrease the probability of crack formation. An advantage associated with the ability of slip to spread from primary planes is illustrated in figure 4. In this example the width of the band is much larger than the interatomic spacing. In the elementary case of a simple tilt boundary, it can be seen that if the plastic displacement D is confined to a single plane, the size of the virtual crack produced by bend plane splitting[19] is larger than those generated by the same overall displacement distributed over several slip planes.

In the general case, the site of crack nucleation within the grain boundary impingement zone of a glide band will most probably be an inhomogeneity in the form of a pore or precipitate, since the local net fracture strength is reduced. If the precipitate or particle is sufficiently large, it may itself crack which then causes failure of the surrounding matrix as discussed by McMahon and Cohen[20]. Although it is recognized that particle effects are very important, we shall not consider them explicitly in order to focus attention on the role of slip character.

The influence of the ease of cross slip and the number of slip systems upon fracture are difficult to analyze rigorously. The ultimate solution of this problem lies in being able to calculate the magnitude of local stress concentrations in the strain hardened state. Until this is accomplished the approximate approach of Armstrong et al is useful because it involves parameters that can be experimentally determined, namely the flow stress at a given strain and the Hall-Petch slope k* obtained at the same strain.[21]

*The slope k of the tensile flow stress-strain size relationship is given by $k = mk_s$.

It can be shown[22] that the condition for crack formation can be expressed by the fundamental equation

$$\sigma\, nb \geq A\, \gamma \qquad (2)$$

where σ = applied tensile stress
nb = plastic displacement of a blocked shear zone or band equivalent to a pile up of n dislocation of Burger's vector b
γ = energy dissipated per unit area of crack surface
A = a constant

In the solids of interest to us here, namely, single phase polycrystals free from interstitial locking effects which are important in steels, the stress strain curves are generally smooth without Lüders band formation. In ionic solids and bcc metals[21], the stress to form a crack is more than that necessary for propagation to complete failure. No evidence has been obtained to suggest that stable cracks are formed in a uniaxial tensile test at stresses much lower than the fracture stress, in contrast to the situation in steels where included carbides, etc., provide sites for premature crack initiation, McMahon and Cohen[20]. Therefore, the above expression represents in principle the condition for fracture. If crack forms at small plastic strains nb can be written in the approximate form[23]

$$nb \simeq (\tau - \tau_o)^{\ell/\mu} \qquad (3)$$

where μ = shear modulus.

Since

$$\tau - \tau_o = k_s \ell^{-\frac{1}{2}}, \qquad nb = \frac{k_s}{\mu}\, \ell^{\frac{1}{2}}$$

from equation (2)

$$\sigma\, k_s\, \ell^{\frac{1}{2}} \geq A\, \mu\, \gamma \qquad (4)$$

Since k_s is a microscopic measure of grain boundary hardening and is therefore not amenable to experimental measurement, it is necessary to replace k_s by k/m. The method of derivation of the above equation is identical to those used by Cottrell[22] and Petch[24] except that the k parameter is now a function of slip character rather than a function of interstitial locking of dislocation sources. It is important to note that when fracture occurs after about 3-4% plastic strain, the approximate expression (3) is no longer appropriate in that it grossly overestimates nb. Smith and Worthington[25] have analyzed the complementary case wherein the number of slip systems are considered in addition to interstitial locking effects.

An advantage of incorporating a consideration of slip character is that we can appreciate the role of solute elements and temperature in a different and broader context. Hitherto, the introduction of solid solution hardening elements and a decrease in temperature have been thought to encourage crack nucleation simply by decreasing dislocation mobility through the term τ_o. However, it is clear that we must inquire about how these changes also affect the ability to cross slip and hence the slip character.

In ionic polycrystals of the rock salt structure the ductility (plastic strain prior to fracture) increases rapidly in that temperature range of transition in slip character from planar to wavy glide. Primary {110} glide bands grow by the multiple cross slip mechanism in which screws cross slip on secondary {100} planes. At low homologous temperatures, bands are intensely planar -- with very high dislocation density. Indications are that screws move only to a very limited extent on the appropriate {100} cross slip plane before they then spread extensively on a parallel {110} plane. The total area swept out by dislocations on {110} planes is far in excess of that on {100} planes, therefore, to a first approximation the Von Mises criterion is not obeyed. As the temperature is increased, dislocation mobility on {100} cross slip planes increases and screw dislocations move further before moving back on a primary (110) plane and the slip bands get more diffuse. There is a temperature regime in which the proportion of {100} slip is gradually increased, so that strain compatibility can be satisfied to an increasing extent. If slip could occur with equivalent freedom on both {110} and {100} planes, then there would be five independent systems and the polycrystalline aggregate would be ductile. In terms of slip topography there is transition from planar to wavy glide. For example, when bromine ions are introduced substitutionally in KCℓ polycrystals, there is some solid solution hardening but the most striking consequence is the increase in temperature at which the slip mode changes (by restricting {100} slip) with the corresponding increase in the ductile-brittle transition temperature[2].

The effect of changes in the state of order in an equi-atomic iron cobalt solid solution containing 2% vanadium has been considered by Johnston et al[21] who find similar correlations between slip character and fracture behavior. The iron cobalt alloy is a useful one for study because the wide variation in degree of order which can be obtained, produces large changes in the initial flow stress and in slip character. Moreover, this system does not mechanically twin before or during fracture at the temperature relevant to the transition behavior. Finally, since the interstitial elements are removed from solution by the vanadium their effects are minimized. The contrast between the respective ductile-brittle transition of disordered and ordered material is shown in figure 5. Again a correlation of fracture behavior with slip character

transition was found: in disordered material, deformation occurred exclusively by wavy glide at temperatures down to -100°C below which planar glide bands began to appear. The ordered material deformed by planar glide at all temperatures up to 450°C. A further significant aspect of the behavior of iron cobalt was the fact that throughout the entire temperature range, the initial flow stress ($\epsilon \sim .02$) of ordered material was 30 - 50% less than the disordered alloy, as illustrated in figure 6. In this example, therefore, the consequences of the changes in slip behavior outweigh those of changes in initial flow stress.

Another example of a lack of correlation between initial flow stress and ductile-transition is afforded by the effects of adding vanadium to low-carbon iron.[6] As already pointed out, increasing vanadium content progressively restricts cross slip which causes a transition to occur from dislocation cell formation to the generation of a uniform distribution of long straight segments (i.e., within glide bands). From figure 7 it can be seen that there is progressive increase in ductile-brittle transition temperature at the vanadium content is increased. In contrast, the yield stress passes through a minimum as vanadium is added, as shown in figure 8, this softening effect is considered to be due to the removal of interstitials from solution in the form of coarse particles of a vanadium compound.

Each of the above examples are interpreted to show that changes in slip behavior that accompany increased difficulty of cross slip increase the tensile flow stress by rapid strain hardening through an increased value of k_s. The condition for crack formation given by equation $\sigma k_s \ell^{\frac{1}{2}} \geq A$ is therefore satisfied at a lower value of plastic strain ϵ.

SLIP CHARACTER AND FATIGUE

In the previous section we have discussed the influence of slip character on fracture behavior under unidirectional loading conditions. In this section we will be concerned with the extent to which slip character affects fracture under cyclic loading conditions. For convenience the subject will be considered first with respect to the crack initiation stage and then with respect to crack propagation.

Crack Iniation. Attention will be confined to the mode of crack initiation which involves the formation of a notch-peak topography within the slip bands generated during cyclic loading. It is known that cracks which originate at the stress-raisers created in these bands, grow at first along the slip bands and then at right angles to the tensile stresses as indicated in figure 9.[3][26] As pointed out above,

the nature of the bands is strongly dependent upon slip character; and the notch-peak topography ranges from a very irregular form in materials which cross-slip readily, such as copper[27] and iron[7] (figure 9a), to a much more regular form in materials wherein cross slip is difficult, such as Cu-7Al[28] and Fe-3Si[7] (figure 9b). The development of this topography appears to be an essential feature of the fatigue process, and requires the coordinated motion of many dislocations in order to create sharp surface discontinuities. In materials wherein the slip character is such that the high stress concentrations at slip bands are not easily developed, the resistance to fatigue is extremely high. Examples of such materials are single crystals of MgO[29] and LiF[3] and also zinc[30] crystals that are oriented for single slip and tested at 78°K. In each of these cases there is very limited slip on the cross slip system, and although a screw dislocation can easily move out of the primary glide plane, the edge segment which develops on the secondary plane is relatively immobile. This segment interferes with further slip locally and forces the slip band to widen rapidly, with the result that no sharp notch-peak topography is developed.

Crystals of this type exhibit another important characteristic in that they harden to such a remarkable extent under cyclic loading conditions that the initial flow stress can be increased by a factor of 10. This hardening behavior is thought to result also from the difficulty in cutting through the immobile edge segments within the glide bands by other screw dislocations of the same Burger's vector. In these materials the fatigue strength at 10^7 cycles is an order of magnitude above the initial flow stress. This fact indicates that the applied stress must be increased considerably before the necessary concentrated to-and-fro motion of dislocations can generate the topography required for crack initiation. In practice, however, static failure usually occurs eventually upon an increase of load, and the surface topographical features are never marked.

From these examples we see that two interrelated aspects of fatigue, namely the nature of the topography and the degree of hardening are a function of the nature of the slip process involved. Since the glide-band notch-peak severity decreases with increasing difficulty of cross slip, is there not always a marked increase in fatigue resistance as the ability to cross-slip decreases? At a given stress level and grain size this is generally true, but measured in terms of the yield strength (0.2% offset) of polycrystalline material there may not be any particular gain. In fact for copper base alloys tested at room temperature, irrespective of stacking fault energy and hence of slip band topography, the fatigue strength at 10^7 cycles is approximately equal to the yield strength[31] The yield strength depends upon the attainment of a stress level sufficiently high so that rapid dislocation multiplication through a multiple cross glide process can occur. Apparently this same condition must be met in

order for the fatigue slip bands to develop, and in the absence of any marked cyclic hardening, as will be discussed, these two levels are approximately equal. Below the stress corresponding to 10^7 - 10^8 cycles, although fine slip can occur, the effects are non-damaging since the concentrated cyclic motion of dislocations within glide bands does not take place.

While it is true that the stress corresponding to a life of 10^7 cycles of these copper base alloys is equivalent to their yield strength, there are other materials for which the endurance limit is much higher than the yield strength, for example the LiF which has already been mentioned. The ratio of fatigue strength (10^7 cycles) to yield strength for a number of materials is given in Table II. We see for the f.c.c. metals copper and its alloys, aluminum, and nickel that the ratio is close to unity. On the other hand, for b.c.c. iron and for disordered Ni_3Mn (f.c.c.), the endurance limit is almost 50% higher than the yield strength. The aforementioned hardening behavior of MgO and LiF suggests that a correlation between the degree of cyclic hardening and the fatigue strength of these materials may exist. To ascertain if this is so, the cyclic load-deflection curves for a number of materials were determined. The extent of cyclic hardening was measured by cycling between fixed deflection limits until a saturation value of load for a particular deflection amplitude was reached. Once a saturation value had been determined, the amplitude was increased and the value characteristic of the new amplitude determined. These results are shown in figures 10 to 13, and are compared to the unidirectional load-deflection curves. The specimens used in these experiments were cantilever beams about 0.050 inches thick which contained a uniform moment section. The cycling was carried out in an Instron machine equipped with an automatic chart recorder. The amplitudes were increased gradually and saturation was usually obtained in less than 100 cycles after each incremental amplitude increase.

The curves shown for copper are similar in nature to others obtained for aluminum and copper base alloys. For the copper base alloys the degree of hardening decreased with decrease in the stacking fault energy in accord with the observations of Avery and Backofen[28] and Strutt[34]. The fact that the degree of cyclic hardening is lower the lower the stacking fault energy is in contrast to unidirectional behavior. As pointed out by Feltner[35], cyclic hardening is facilitated by ease of cross slip, whereas, as indicated earlier, unidirectional hardening is promoted by a difficulty in cross slip.

It should be noted that for copper both the unidirectional and the cyclic curves deviate from the initial straight line at about the same stress level, i.e. the initial flow stress has not been significantly altered by cycling. In contrast, the cyclic hardening curve for iron shows a marked increase in resistance to plastic deformation in this region. These results suggest that where such marked hardening

occurs, the plastic deformation required for slip band topographical effects is not available and hence the fatigue strength to yield strength ratio is raised. The reasons for the marked hardening in iron in contrast to copper are not clear. The fact that slip is generally more wavy in iron and more slip systems are available, certainly suggests that ease of cross slip may be a factor. Yet transmission microscopy studies of the internal structure developed on cycling reveal no great difference. The carbon content of the iron was of the order of 100 ppm and strain aging may be a factor. For example, resting a specimen for a period of 72 hours after cycling to saturation at a fixed amplitude resulted in a 14% increase in load amplitude upon initial recycling. Some softening occurred upon further cycling, but at least 10% of the increment was retained.

It is noted that the other materials in Table II which exhibit a fatigue strength to yield strength ratio greater than unity also exhibited a high initial degree of cyclic hardening. For example, in three of the four cases shown in figs. 12 and 13, the materials harden considerably at low values of plastic strain. This hardening results in a marked decrease in the plastic strain amplitude and an increase in the fatigue strength relative to the yield strength. The hardening of the ordered alloys is thought to be due to the non-coordinated cross slip of the super dislocations leading to the creation of anti-phase boundaries. However, the cause of the hardening of the disordered Ni_3Mn alloy which exhibits planar glide is not clear. In the fourth case, the disordered FeCo-V alloy, which exhibits wavy glide, the alloy actually softens slightly. For both of the nominally disordered alloys a degree of order may in fact be present which is responsible for the observed behavior. We note also that in the case of the ordered FeCo-V, cyclic load deflection curves are affected by whether or not a yield drop occurs prior to cycling. If the load is increased slowly from below the yield region, and if the surface is lightly abraded to introduce additional dislocation sources, then the cyclic load-deflection curve remains close to the extension of the initial load-deflection line. However, if on the first application of load the yield is exceeded, then a sharp yield drop occurs and a large number of dislocations is introduced. The cyclic load-deflection curve is then displaced to a larger amplitude, and the slope is less steep.

As has been discussed by Manson[36], Morrow[37], and Alden[38] the cyclic stress-strain properties markedly influence the fatigue behavior in the finite life range. We see from the cyclic hardening response of Ni_3Mn, figure 12, at a given load level the plastic amplitude is greater in the case of the disordered material, and we therefore expect that at any given stress level the life of the disordered should be less than the ordered condition. Further, the rate of increase of plastic strain amplitude is less in the case of the ordered alloy than for the disordered alloy. We therefore expect that the slope of the S-N curves for the ordered condition to be higher than that for disordered material.

Examination of the S-N curves obtained by Boettner et al[4] for these conditions, figure 14, reveals that the experimental findings are in accord with these expectations. It is also noted that only in the case of iron, figure 11, is there a relatively sharp break in the cyclic load-deflection curve. This suggests that the existence of a well-defined knee in the S-N curve may be related to this type of hardening behavior.

These studies of homogeneous, single phase materials serve to underline the fact that although the cyclic hardening response is related to the nature of the slip process, there are cases, e.g., iron, in which the factors responsible for the degree of hardening are not yet fully understood. It is appropriate to draw attention to the fact that many technically important materials such as high strength aluminum alloys and steels exhibit fatigue strengths at 10^7 cycles well below the macroscopic yield strength of the alloys. In such heterogeneous alloys, concentrated slip can occur in localized regions below the macroscopic yield level and thereby reduce the fatigue strength.

Crack Propagation. The process of fatigue crack propagation can be divided into two stages as indicated in figure 9. In the first stage (I) the fatigue crack advances along the initiating slip planes. In the second stage (II) the crack propagates macroscopically at right angles to the tensile stress. Relatively little is known about the mechanism of growth in the stage I, but stage II has been studied in some detail, and it is with this stage that we will be primarily concerned.

In stage II the crack advances an increment in each cycle, with the characteristic ripple markings on the fracture surface indicating the successive positions of the crack front. As shown by Laird and Smith[39] these markings arise as a result of the blunting and resharpening of the crack tip during the loading cycle. Slip character in this stage primarily affects the degree of strain hardening at the tip of the growing crack. For materials in which strain hardening is high there will be a tendency for the plastic zone at the tip of the crack to spread laterally and thereby blunt the crack tip, leading to the arrest of the forward progress of the crack in each cycle. In materials of low strain hardening, this lateral spread is minimized with the result that for a given displacement of the walls of the crack the tip remains sharper than for a high-strain hardening material and propagates further in each cycle.

To assess the role of stress in fatigue crack propagation it is convenient to use sheet specimens and observe directly the crack length as a function of the number of load cycles. From this information a rate of crack growth can be determined. When plotted as a function of a stress intensity parameter σ_g/ℓ in log-log coordinates where σ_g is the peak gross stress and ℓ is the semi-length of an internal crack, it

is found that the rate is approximately a single valued function of this parameter.[40][31] An example of such a plot of results[41] for 7075-T6 aluminum sheet 12 inches wide is shown in figure 15, for the case of approximately zero minimum stress in the loading cycle (R = 0). it is noted that the data curve (a) is not a straight line. At lowest rates an asymtotic value of $\sigma_g\sqrt{\ell}$ is approached which in this case is 1480 lbs. in.$^{-3/2}$, and at the highest rates where the net section stress is sufficient to cause general yielding, a considerably higher rate is observed. However, over much of the range where the net section stresses are elastic the curve (a) can be approximated by a straight line of slope 4,[42][31] (although in certain limited regions perhaps another value for the slope would be more appropriate). Theoretical support for a dependence on the fourth power of $\sigma_g\sqrt{\ell}$ has recently been given by Weertman[43], McClintock[44], and Kraft [45]. A simple power approximation has the advantage that it allows comparisons and computations to be made in a straightforward manner. Curve (b) of figure 15 is included to show that if one supposes that a critical value of the parameter $\sigma_g\sqrt{\ell}$ must be exceeded before crack growth occurs, which in this case is taken to be 1480 lbs. in.$^{-3/2}$, then a plot of the data in terms of the excess over this critical amount differs from curve (a) considerably at low rates of crack growth. However, in terms of the nature of the crack growth process there is no significant change observed in the mode of crack growth that correlates with the change from the flat to the steep portion in this type of plot.

For the present we will assume that the fourth power approximation holds where the net section stress is elastic. If we integrate the equation

$$d\ell/dN \propto \sigma_g^4 \ell^2 \qquad (5)$$

we expect that the fatigue lifetime of sharply notched sheet specimens should vary inversely as the fourth power of the applied stress, since in this case most of the lifetime is spent in stage II crack propagation. A comparison with experimental results is shown in figure 16 for two sharply notched aluminum alloys of three different widths. We note that the slope is close to the expected value over most of the range. The experimental slope is less than $\frac{1}{4}$ at both the high and low stress levels in accord with observed changes in the growth rates in these ranges. That the total lifetime is independent of width is a reflection of the fact that most of the lifetime is spent where the cracks are small and insensitive to finite width effects.

As the cracks advance in sheet specimens, an obvious manifestation of strain hardening behavior can be observed. The cracks grow initially in stage II along a plane normal to the direction of tensile loading. After some distance which is a function of stress level, the plane of separation shifts to a 45° orientation with respect to the thickness direction of the sheet. The region of transition has been related to the size of the plastic zone at the crack tip, with the transition itself related to the distance at which the plastic zones extend through the sheet thickness.[46] The first part of the growth is in plane strain, whereas, after the shift plane stress conditions

prevail. Let us inquire as to the relative rate of growth under these two conditions. Integration of Eq. (5) between the limits $\ell = \ell_o$ and $\ell = \ell$ leads to the relation

$$N \propto \frac{1}{\sigma_g^4}\left(\frac{1}{\ell_o} - \frac{1}{\ell}\right) \qquad (6)$$

For a fixed value of σ_g, the number of cycles for a given value of ℓ versus the parameter

$$\left(\frac{1}{\ell_o} - \frac{1}{\ell}\right)$$

should plot as a straight line. Figure 17 indicates the results of an analysis of data for two aluminum alloys at σ_g = 20 ksi treated in this manner. We see that indeed straight lines describe the data in the early stage, but that a break occurs as the cracks grow in length. This break corresponds to the shift from plane strain to plane stress. It occurs at a smaller crack length in the 2024 alloy because its lower yield and higher work hardening rate result in a larger plastic zone at a given crack length. Examination of this figure also indicates that the cracks grow more slowly in plane stress than in plane strain, although this difference is not pronounced when the data is plotted in a log-log plot of the type shown in figure 15. Direct evidence for this difference is given in these alloys by the fact that the crack front is curved, with the plane stress region at the surface lagging the plane strain region in the interior. The reason for this difference appears to result from the fact that the imposed deformation must be assimilated by the immediate vicinity of the crack tip in the case of plane strain, whereas in plane stress with larger amounts of accompanying plastic strain the imposed deformation can be assimilated to a greater extent by the larger plastic zone, thereby imposing less of a local strain on the tip itself.

The fourth power relationship may be used as a general approximation to compare the behavior of a variety of alloys as shown in figure 18. It is seen that for a given value of $\sigma\sqrt{\ell}$ that a considerable range in resistance to fatigue crack growth exists. What are the factors which determine the relative position of these curves? A guide in this matter is provided by Weertman's analysis[43] which indicates that in a non-strain hardening material the rate of growth is given by

$$\frac{d\ell}{dN} \propto \frac{\sigma_g^4 \ell^3}{\mu\gamma\sigma_y^3} \qquad (7)$$

Here μ is the shear modulus, γ is a Bilby-Cottrell-Swindon[47] surface work term, and σ_y is the yield strength. We also know that the increment of crack growth per cycle involves a highly localized plastic deformation process as the crack tip blunts and resharpens during each loading cycle as shown in figure 19. It is noted that the serrated nature of the cracked surface results from a sliding off process which alternates between the two plastic zones at the crack tip. Inasmuch as the material at the crack tip is not cycled for many cycles at the peak local value during propagation, we consider that this process of separation is primarily a unidirectional process and as such is governed by the conventional tensile behavior of the material. If the plastic deformation process is considered to be a plastic instability phenomenon[45], then we can relate the peak local stress to the tensile strength of the material which is also governed by an instability process, and therefore replace σ_y by σ_u in the Weertman expression. In addition, the γ term represents the work of separation, which we take to be equivalent to the area under the stress-strain curve up to the tensile strength and, therefore, includes the beneficial effects of strain-hardening. Thus γ can be approximated by the quantity

$$\gamma \approx \left(\frac{\sigma_y + \sigma_u}{2} \right) \varepsilon_u \qquad (8)$$

where ε_u is the strain at the tensile strength. We replace the shear modulus, μ, by Young's modulus, E, and eq. (7) then becomes

$$\frac{d\ell}{dN} \alpha \frac{\sigma^4 \ell^2}{\left(\frac{\sigma_y + \sigma_u}{2} \right) \varepsilon_u \sigma_u^2 E} \qquad (9)$$

The data of figure 18 when plotted against the parameter

$$\frac{\sigma\sqrt{\ell}}{\left[\left(\frac{\sigma_y + \sigma_u}{2} \right) \varepsilon_u \sigma_u^2 E \right]^{\frac{1}{4}}}$$

are shown in figure 10. Except for the 7075 aluminum alloy the data fall in a narrow band indicating that the above parameter is useful in rationalizing the behavior of these materials and in effecting a reasonable correlation. The exceptional behavior of the 7075 material may be due to the destruction of the GP zones by dislocation cutting facilitated by the concentration of deformation at the crack tip as a result of the material's low work hardening capacity. Such a process would lower the value of σ_u locally and account for the discrepancy.

One important aspect of this analysis is that it points out that alloys of much greater resistance to crack growth cannot be anticipated because large increases in unidirectional strength result in such smaller increases of the controlling parameter. The results also indicate that so long as the alloys remain stable an estimate of the rate of growth as a function of temperature may be made if the appropriate stress-strain and modulus values are available.

In this analysis the effects of slip mode have not been explicitly discussed. However, they are present in controlling the unidirectional strain hardening rate which affects the area under the stress-strain curve and the value of σ_u. It is emphasized that the unidirectional properties of the material as influenced by slip behavior are of paramount importance in crack propagation, whereas in the initiation stage, especially at low stress levels the effects of slip mode on cyclic hardening must be taken into account.

Thus far we have considered only cracks initiated at stress raisers, in which case almost the entire lifetime of the specimen is spent in crack growth. It is of interest to know just what portion of the lifetime is spent in growth and what portion is spent in initiation for unnotched specimens. We approach this problem by considering two ranges of applied strain. In one case we consider the range leading to low cycle fatigue, and in the other we consider those materials which exhibit fatigue failures below the yield strength such as steels and aluminum alloys and for which the 4th power approximation can be used to describe the rate of crack growth.

Experimental studies in the low cycle range with unnotched specimens show that crack propagation occupies a major portion of the total lifetime, although for most of this crack growth period the cracks may be quite small.[48] It is the similarity in the nature of the deformation at the crack tip which accounts for the fact that so many ductile materials exhibit about the same lifetime as a function of large plastic strain amplitudes. A relationship between the applied strain range, ε_r , and the fatigue lifetime can be obtained on the basis of crack propagation as follows. Figure 21 shows the results of an experimental determination using electron and light microscopy to determine the spacing of ripples on the fracture surface of copper specimens as a function of a strain intensity parameter, $\varepsilon_r\sqrt{\ell}$. In this range the experimental results indicate the rate of crack growth is given by

$$\frac{d\ell}{dN_R} \alpha \varepsilon_r^2 \ell, \qquad (10)$$

where N_R is the number of cycles spent in the ripple stage of growth (stage II). If we assume that the stage II of growth starts where the strain intensity factor $\epsilon_r\sqrt{\ell}$ at the base of a notch created by slip reaches a critical value $(\epsilon_r\sqrt{\ell})_1$, and that final fracture occurs where another critical value $(\epsilon_r\sqrt{\ell})_2$, is reached, then:

$$(\epsilon_r\sqrt{\ell})_1 = C_1 \tag{11}$$

$$\text{for a fixed } \epsilon_r,\ \sqrt{\ell_1} = \frac{C_1}{\epsilon_r} \text{ or } \ell_1 = \frac{C_1^2}{\epsilon_r^2} \tag{12}$$

$$\text{and similarly } \ell_2 = \frac{C_2^2}{\epsilon_r^2} \tag{13}$$

Upon separation of the variables in (10) and integrating between the limits of ℓ_1 and ℓ_2 we obtain

$$\epsilon_r^2 N_R \propto \ell_n \frac{C_2}{C_1} = C_3 \tag{14}$$

Now we know from experimental determination that for lives less than 10^3 cycles, almost the entire lifetime N_T is spent in stage II growth. We, therefore, substitute N_T for N_R to obtain the result that

$$\epsilon_r^2 N_T \propto C_3 \tag{15}$$

which is the expression found by Manson[49] and Coffin[50] to describe the behavior of ductile materials in the low cycle range. Again, the fact that many metals and alloys exhibit the same fatigue behavior in this range is thought to stem from the fact that the geometrical aspects of crack tip deformation are similar in this class of materials.

As the strain amplitude is decreased so that cycling takes place in the nominally elastic range where the fourth power approximation can be used, the rate of crack growth is given by

$$\frac{d\ell}{dN} \propto \sigma_g^4 \ell^2 \tag{5}$$

As above, we consider stage II propagation to occur between an initial critical value of $(\sigma\sqrt{\ell})_1$ and a final value $(\sigma\sqrt{\ell})_2$. Integrating in a manner as above leads to the relation

$$N_R \propto \frac{1}{\sigma_g^2} \tag{16}$$

This result indicates that the number of cycles spent in stage II crack propagation in an unnotched specimen varies inversely only as the 2nd power of the stress level. However, the total life may vary inversely by as much as the 10th power. Hence we conclude that the life spent in crack growth (stage II) at low stresses is but a small portion of the total lifetime, which is in accord with experimental observations[51]. Most of the lifetime of unnotched specimens stressed near the endurance limit is spent in slip band formation and growth along the slip planes (stage I); $N_R \ll N_T$*.

This is not to say that at these levels in unnotched specimens that crack growth is unimportant. The presence of flaws can bring about a situation whereby the critical value $(\sigma\sqrt{\ell})_1$ is exceeded and growth can begin almost immediately. An example of such an effect is shown in figure 22, for a high strength constructional steel.[52][53] It is seen that the flaws present in the as-received condition markedly lower the fatigue resistance of this high strength alloy. The slope of the line for this condition above the knee of the S-N curve is such as to suggest that cracks were quickly initiated and most of the lifetime was spent in propagating these cracks to failure.

*If we substitute ϵ for σ_g in this nominally elastic range, we see that over both the elastic and plastic ranges that the number of cycles in stage II varies inversely as the square of the strain amplitude.

SUMMARY

1. Slip character may be considered in terms of slip band appearance, dislocation arrangement and configuration. The important features are the number of slip systems and the ability to cross slip.

2. A smaller number of slip systems and a decreased ability to cross slip enhance the effect of grain size on the micro and macroscopic stages of unidirectional strain hardening and in so doing increase the flow stress of polycrystals.

3. Changes in the number of operable slip systems and the ability to cross slip brought about by alloying and temperature are important in determining the transition from brittle to ductile behavior.

4. Slip character affects the nature of the cyclic hardening process and thereby the stress level at which cracks are initiated within the glide bands; these features are reflected in the slope of the S-N curve. In contrast to its influence upon brittle-ductile behavior, planar glide improves the fatigue properties.

5. Crack growth in the ripple stage occupies less of the total lifetime as the strain amplitude is reduced. The growth process in this stage is governed by the unidirectional properties of the material. The parameters determining the resistance to growth are the modulus, the area under the unidirectional stress-strain curve, and the tensile strength of the material.

References

1. Stokes, R. J. and Li, C. H., Symposium, "Structure and Properties of Engineering Materials," Raleigh, North Carolina, March, 1962.
2. Stoloff, N. S., Lezius, D. K. and Johnston, T. L., J. Appl. Phys. 34, 3315, 1963.
3. McEvily, A. J. and Machlin, E. S., "Fracture," Averbach, B. L., Felbeck, D.K., Hahn, G. T. and Thomas, D. A. Eds., Wiley, New York, 450, 1959.
4. Boettner, R. C., Stoloff, N. S. and Davies, R. G., Trans. AIME (in press).
5. Stoloff, N. S. and Davies, R. G., Acta Met. 12, 251, 1963.
6. Stoloff, N. S. and Davies, R. G. and Ku, R. C., Trans. AIME 233, 1500, 1965.
7. Boettner, R. C. and McEvily, A. J., Acta Met. 13, 937, 1965.
8. Swann, P. R., "Electron Microscopy and Strength of Crystals," Thomas, G. and Jack Washburn Eds., Interscience, New York, 1963.
9. Davies, R. G. and Stoloff, N. S., Phil. Mag. 9, 349, 1964.
10. Davies, R. G. and Stoloff, N. S., Acta Met. 12, 473, 1964.
11. Ku, R. C., McEvily, A. J. and Johnston, T. C., unpublished results.
12. Thomas, G. J., Australian Inst. of Metals 8, 80, 1963.
13. Keh, A. S. and Weissmann, S., Electron Microscopy and the Strength of Crystals," Thomas, G. and Jack Washburn, Eds., Interscience, New York, 1963.
14. Lawley, A. and Gaigher, H. L., Phil. Mag. 10, 15, 1964.
15. Brown, N. and Ekvall, R. A., Acta Met. 10, 1101, 1962.
16. Armstrong, R., Todd, I., Donthwaite, R. M., and Petch, N. J., Phil. Mag. 7, 45, 1962.
17. Carnahan, R. D., Johnston, T. L., Stokes, R. J. and Li, C. H., Trans. AIME 221, 45, 1961.

18. Groves, G. W. and Kelly, A., Phil. Mag. 8, 877, 1963.

19. Orowan, E., Dislocations in Metals, M. Cohen Ed., AIME, 1954.

20. MacMahon, C. J. and Cohen, M., Acta Met. 13, 591, 1965.

21. Johnston, T. L., Davies, R. G. and Stoloff, N. S., Phil. Mag. 12, 305, 1965.

22. Cottrell, A. H., Trans. AIME 212, 192, 1958.

23. Cottrell, A. H., Dislocations and Plastic Flow in Crystals, Oxford, 1953.

24. Petch, N. J., Phil. Mag. 3, 1089, 1958.

25. Smith, E. and Worthington, P. J., Int. Conf. on Fracture, Sendai, Japan, 1965.

26. Forsyth, P. J. E., Proc. of the Crack Propagation Symposium, Cranfield, England, 76, 1961.

27. Wood, W. A., "Fracture," Averbach, B. L., Felbeck, D. K., Hahn, G. T., and Thomas, D. A. Eds., Wiley, New York, 412, 1959.

28. Avery, D. H. and Backofen, W. A., "Fracture of Solids," D. C. Drucker and J. J. Gilman, Eds., Interscience Publishers, New York, 339, 1963.

29. McEvily, A. J. and Machlin, E. S., Trans. AIME 221, 1086, 1961.

30. Fegredo, D. M. and Greenough, G. B., J. Inst. Metals 87, 1, 1958-59.

31. McEvily, A. J. and Boettner, R. C., Acta Met. 11, 725, 1963.

32. Anon., ASM Metals Handbook, American Society for Metals, Metals Park, Ohio 936, 1961.

33. Ferro, A. and Montalenti, G., Phil. Mag. 10, 1043, 1964.

34. Strutt, P. R., J. Australian Inst. of Metals 8, 115, 1963.

35. Feltner, C. E., Phil. Mag. in press.

36. Manson, S. S., Experimental Mechanics 5, 193, 1965.

37. Morrow, J. D. and Tuler, F. R., J. Basic Engineering, Trans. AIME, Series D, 87, 275, 1965.

38. Alden, T., Trans. AIME 224, 1287, 1962.

39. Laird, C. and Smith, G. C., Phil. Mag. 7, 847, 1962.

40. Paris, P. C., Gomez, M P. and Anderson, W. E., The Trend in Engineering 13, 9, 1961.

41. McEvily, A. J. and Illg, W., Nat. Advis. Comm. for Aero., TN 4394, 1958.

42. Paris, P. C. and Erdogan, F., J. Basic Engineering, Trans. ASME, Series D, 85, 528, 1963.

43. Weertman, J., Int. Conf. on Fracture, Sendai, Japan, 1965.

44. McClintock, F. A., "Fracture of Solids," D. C. Drucker and J. J. Gilman Eds., Interscience Publishers, New York, 65, 1963.

45. Krafft, J. M., Applied Materials Research 3, 88, 1964.

46. Liu, H. W., ibid, 3, 229, 1964.

47. Bilby, B. A., Cottrell, A. H., and Swindon, K. H., Proc. Roy Soc. [A] 272, 304, 1963.

48. Boettner, R. C., Laird, C. and McEvily, A. J., Trans. AIME 233, 386, 1965.

49. Manson, S. S., Nat. Advis. Comm. for Aero., TN 2955, 1953.

50. Coffin, L. F., Trans. ASME 76, 931, 1954.

51. Laird, C. and Smith, G. C., Phil. Mag. 8, 1945, 1963.

52. Lutz, G. B. and Wei, R. P., U. S. Steel Appl. Res. Lab. TR, Proj. No. 40112-011(1), July 1961.

53. Munse, W. H., Stallmeyer, J. E. and Rone, J. W., U. of Illinois Report, 1965

54. McEvily, A. J., Boettner, R. C. and Bond, A. P., J. Inst. Metals 93, 481, 1964-65.

55. Donaldson, D. R. and Anderson, W. E., Proc. of the Crack Propagation Symposium, Cranfield, Englad, 375, 1961.

TABLE I

	Easy Cross Slip	Difficult Cross Slip
Dislocation Distribution Configuration	Cellular tangled, heavily jogged	Uniform long straight segments
Slip band Appearance	Diffuse and/or wavy	Sharp and planar
Unidirectional Strain hardening of polycrystals	Low	High

TABLE II

Material	Yield Strength, psi (0.2% Offset)	Fatigue Strength, psi (10^7 Cycles)	Fatigue Strength / Yield Strength	Reference
Copper	7,500	7,000	0.94	(31)
Copper - 30 Zn	18,000	18,000	1.0	(31)
Copper - 5.6 Al	18,900	20,000	1.06	(31)
Copper - 7.3 Al	35,400	30,000	0.85	(31)
Copper - 7.3 Al	10,700	12,500	1.17	(31)
Copper - 6.5 Al - 2.4 Fe	32,800	31,000	0.95	(31)
Aluminum (99.0)	5,000	5,000	1.0	(32)
Nickel	16,300	15,000	0.92	(33)
Iron - 0.2 Ti	18,200	26,300	1.45	(33)
Fe Co-V ordered	31,000	55,000	1.77	(4)
Fe Co-V disordered	49,000	45,000	0.92	(4)
Ni_3Mn ordered	42,000	48,000	1.14	(4)
Ni_3Mn disordered	27,000	39,000	1.44	(4)

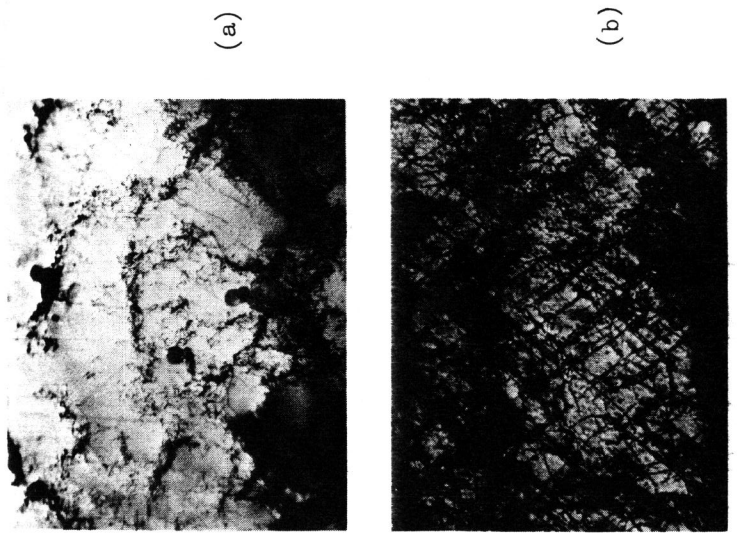

Fig. 2 Contrast between the dislocation distribution and configuration characteristic of materials of a) easy cross slip and b) difficult cross slip for a plastic strain of 6%. 4,700X

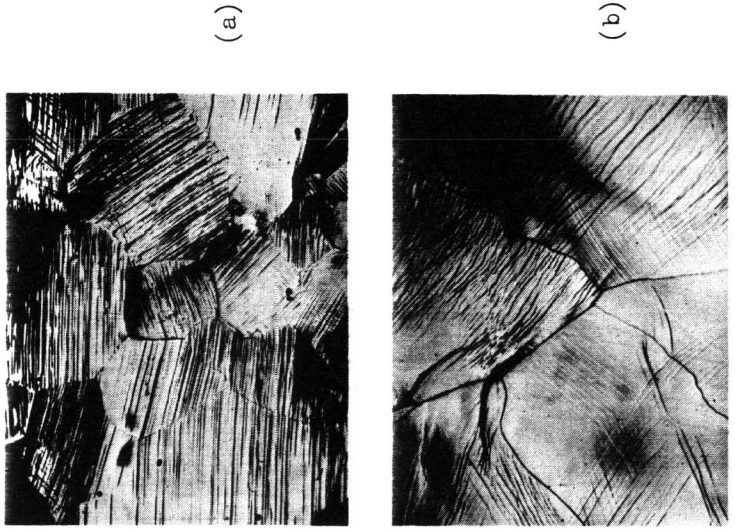

Fig. 1 Comparison of a) planar and b) wavy glide in a deformed crystal. 290X

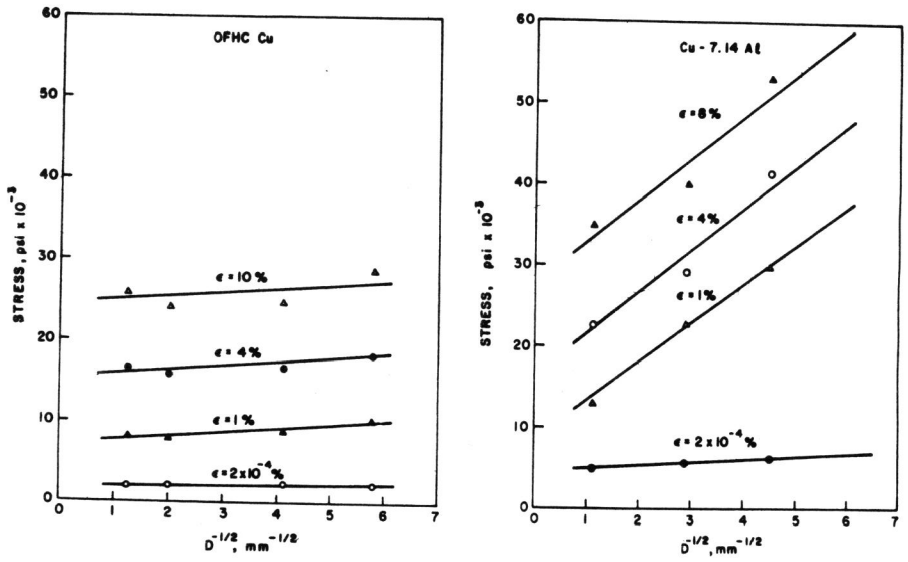

Figure 3. Effect of grain size on the microyield and flow stresses of a) OHFC copper and b) copper - 7.14% Al[11]

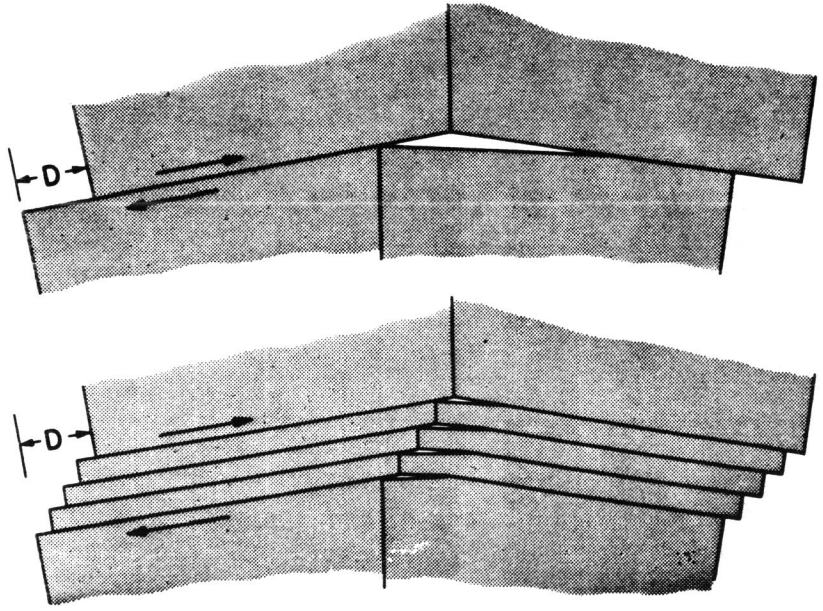

Figure 4. Schematic representation of the strain concentration at a simple tilt boundary as a function of the width of an impinging glide band.

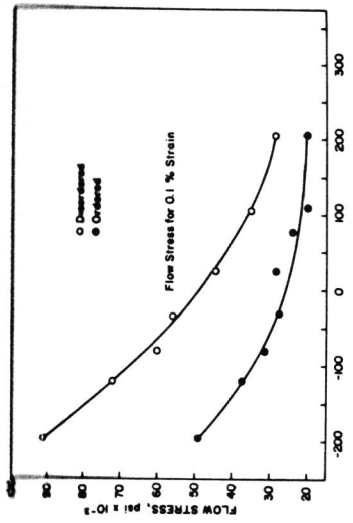

Figure 6. The effect of long range order on the temperature dependence of the macroscopic flow stress (0.1% strain) of FeCo-V[21].

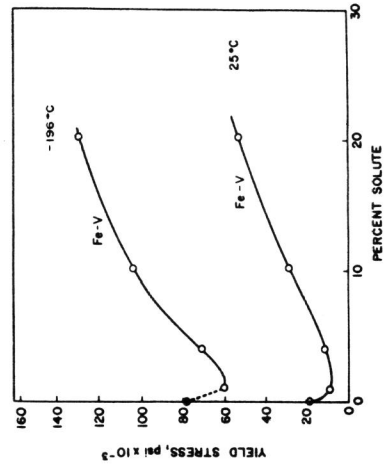

Figure 8. Effect of vanadium on the macroscopic flow stress (2×10^{-3} strain) of iron[6].

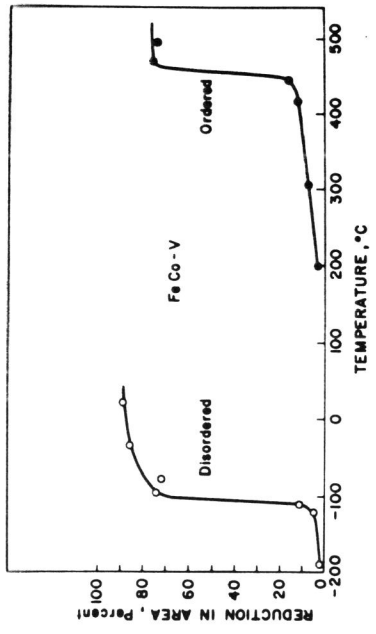

Figure 5. Effect of long range order on the ductile to brittle transition in FeCo-V[21].

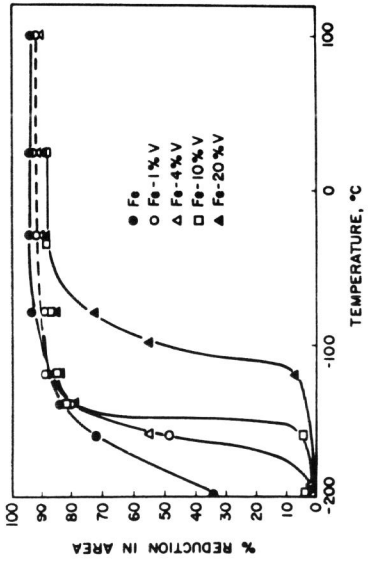

Figure 7. Effect of vanadium on the ductile-brittle transition (6) of iron containing less than 0.01 carbon and nitrogen.

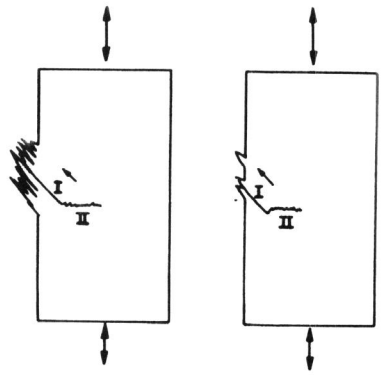

(a) Typical of easy cross slip. (b) Typical of difficult cross slip.

Figure 9. Schematic representations of the types of slip band topography and stages of crack growth.

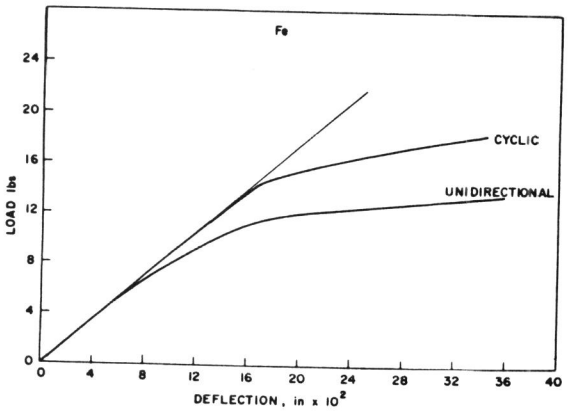

Figure 11. Unidirectional and cyclic load-deflection curves for iron.

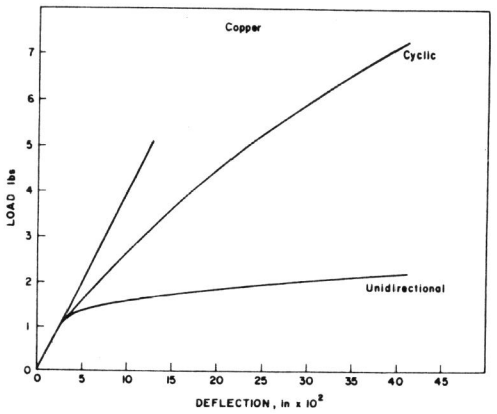

Figure 10. Unidirectional and cyclic load-deflection curves for copper.

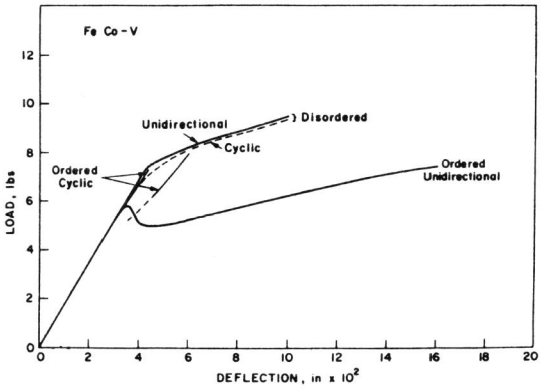

Figure 12. Unidirectional and cyclic load-deflection curves for FeCo-V.

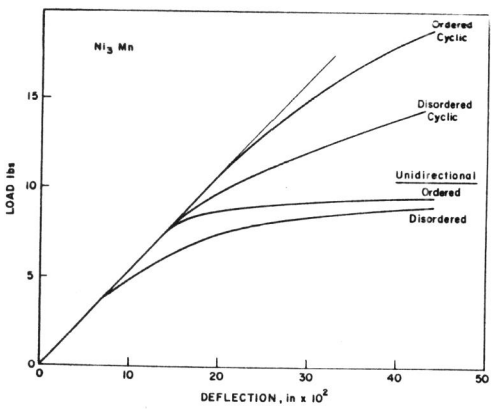

Figure 13. Unidirectional and cyclic load-deflection curves for Ni_3Mn.

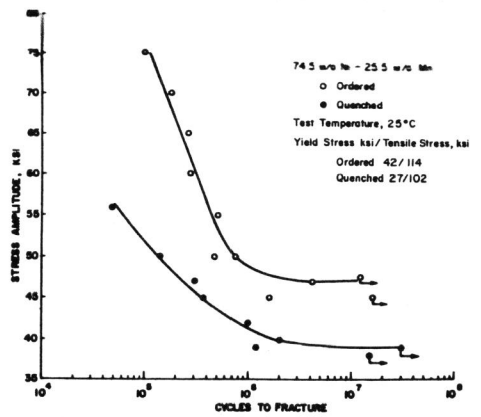

Figure 14. S-N curves for ordered and disordered Ni_3Mn[4].

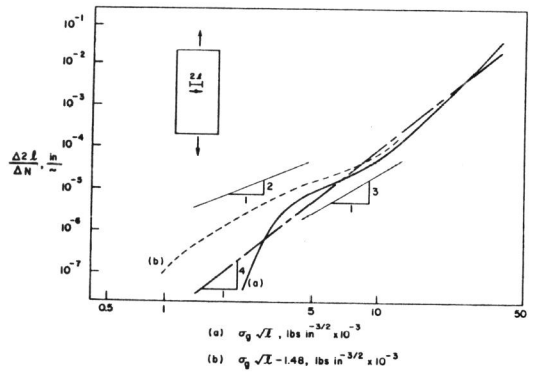

Figure 15. Rate of fatigue crack growth as a function of the stress intensity parameter for 7075-T6.

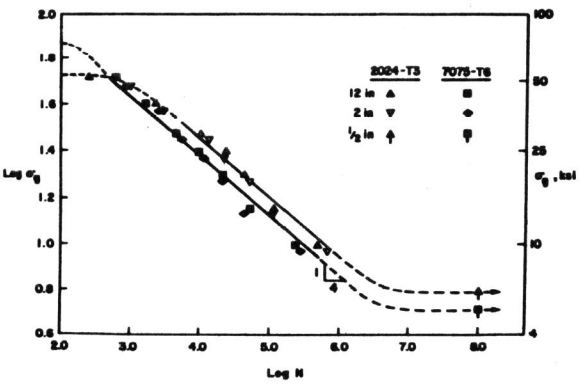

Figure 16. S-N curves for notched specimens of 2024-T3 and 7075-T6.

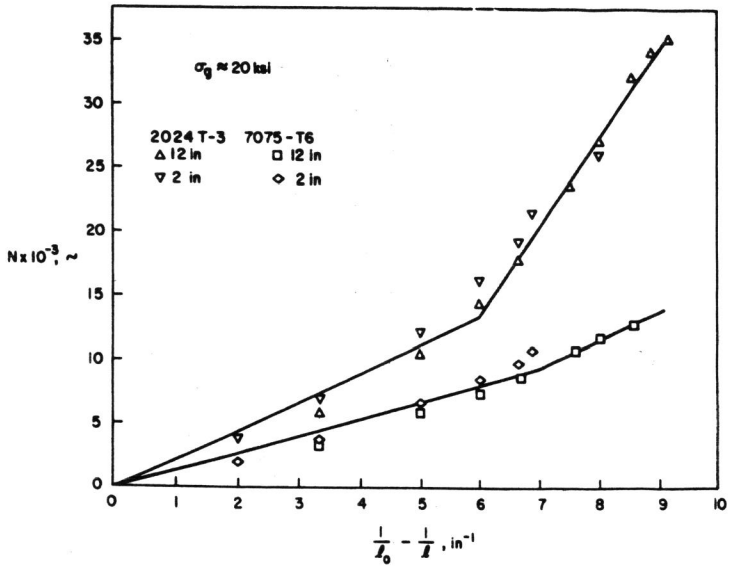

Figure 17. Effect of plane strain and plane stress on fatigue crack growth.

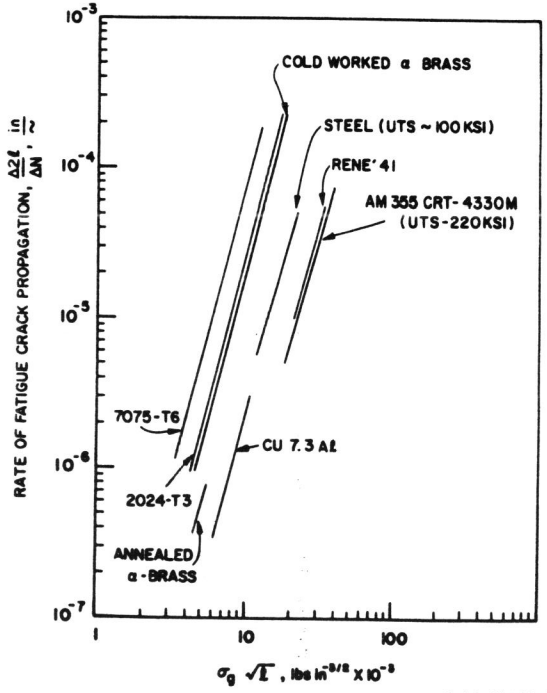

Figure 18. Rate of fatigue crack growth for a number of alloys.[41][31][54][55]

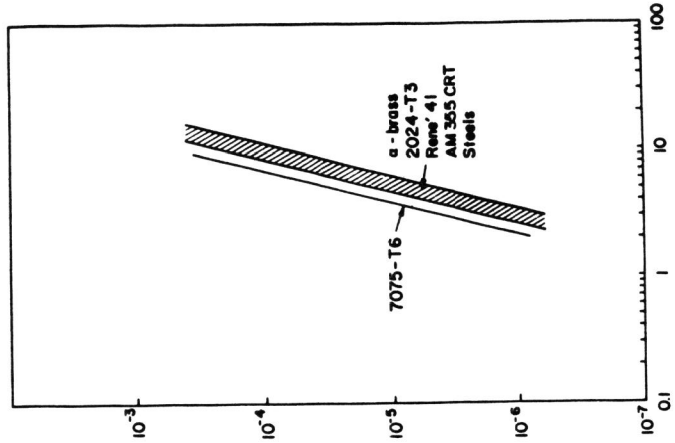

Figure 20. Normalized fatigue crack growth rates for alloys shown in Figure

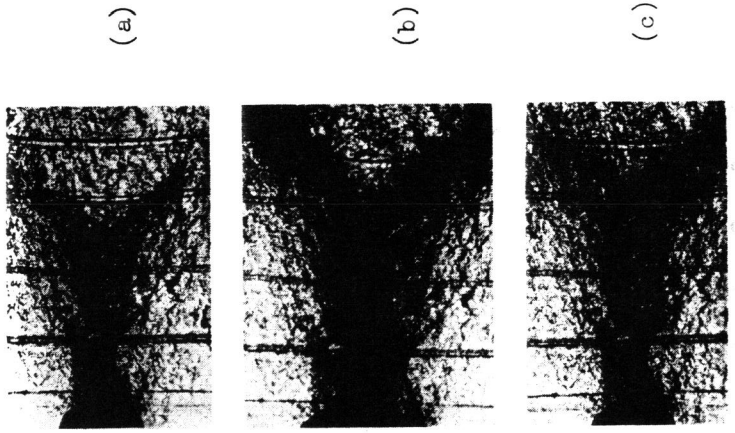

Fig.19 Sequential crack tip deformation during loading cycle. 11X
(a) After compression.
(b) After extension.
(c) After compression.

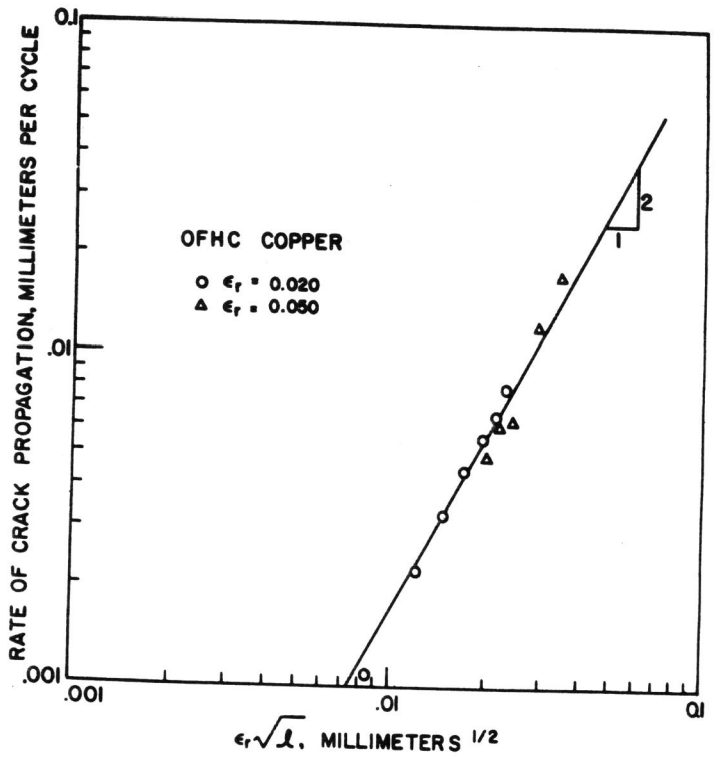

Figure 21. Rate of crack growth in low cycle range as a function of strain intensity parameter, $\epsilon_T\sqrt{\ell}$.

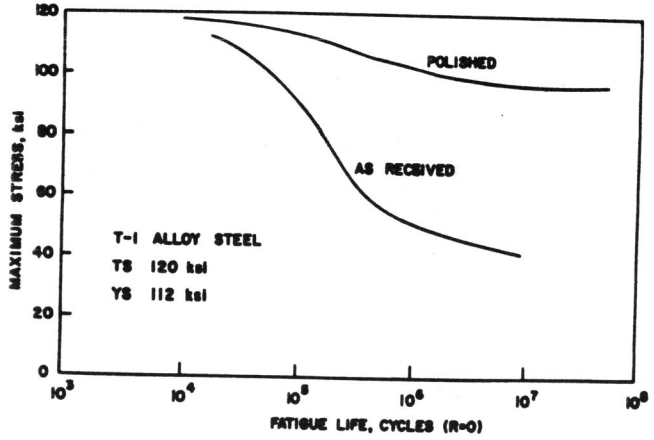

Figure 22. S-N curves for T-1 steel in polished[52] and as-received[53] conditions.